



available at www.sciencedirect.com



journal homepage: www.elsevier.com/locate/jhydrol



Fuzzy-based dynamic soil erosion model (FuDSEM): Modelling approach and preliminary evaluation

Sagy Cohen ¹, Tal Svoray ^{*}, Jonathan B. Laronne ², Yulia Alexandrov ³

Department of Geography and Environmental Development, Ben-Gurion University of the Negev, Beer-Sheva 84105, Israel

Received 24 July 2007; received in revised form 7 February 2008; accepted 7 April 2008

KEYWORDS

Erosion;
Modelling;
Catchment scale;
Fuzzy-logic;
Semi-arid;
Geomorphology

Summary Soil erosion models have advanced in recent years, by becoming more physically-based, with better representation of spatial patterns. Despite substantial progress, fundamental difficulties in catchment scale applications have been widely reported. In this paper, we introduce a new catchment scale soil erosion model. The model is designed for catchment interface and management purposes by: (1) using relatively common input data; (2) having a modular model structure; and (3) a clear and easily interpretable output analysis, by producing possibility or potential, rather than quantitative erosion maps. The model (named: FuDSEM; fuzzy-based dynamic soil erosion model) is spatially explicit and temporally dynamic and is formalized and based on fuzzy-logic equations. FuDSEM was initially evaluated on a small data-rich catchment and was found well calibrated. It was then implemented on a medium-sized heterogeneous catchment in central Israel. Initial evaluations of the medium-scale model predictions were conducted by: (1) comparison of FuDSEM runoff predictions against measured runoff from five hydrological stations and (2) a site specific evaluation of the FuDSEM multi-year erosion prediction in two sub-catchments. FuDSEM was compared with two other erosion models (a temporally static version of itself and a known physically-based model). The results show the advantages of FuDSEM over the other two models in evaluating the relative distribution of erosion, thereby emphasizing the benefits of its temporally dynamic and fuzzy structure. © 2008 Elsevier B.V. All rights reserved.

^{*} Corresponding author. Tel.: +972 86472018; fax: +972 86472821.
E-mail addresses: sagy.cohen@newcastle.edu.au (S. Cohen), tsvoray@bgu.ac.il (T. Svoray), john@bgu.ac.il (J.B. Laronne), julyaa@bgu.ac.il (Y. Alexandrov).

¹ Present address: School of Engineering, The University of Newcastle, Callaghan, New South Wales 2308, Australia. Tel.: +61 24925816; fax: +61 249216991.

² Tel.: +972 86472016; fax: +972 86472821.

³ Tel.: +972 86477652; fax: +972 86472821.

Introduction

Soil erosion modelling is an important tool for viable conservation of natural, agricultural and built-up environments. Catchment-scale erosion modelling is particularly desirable, since it facilitates more efficient soil conservation planning (De Jong et al., 1999) by providing spatial data over large areas, data that may be used to decrease erosion related

problems (Jetten et al., 2003). The potential of such models for environmental management and planning organizations is clear, but most state-of-the-art soil erosion models are difficult to apply over large areas, due to intensive labour and detailed data requirements (Merritt et al., 2003).

Several large scale erosion models, such as WEPP (Nearing et al., 1989), EUROSEM (Morgan et al., 1992), LISEM (De Roo et al., 1996), EROSION3D (Schmidt et al., 1999) and MEDRUSH (Kirkby and McMahon, 1999) have been reported and examined. Despite their important contribution to understanding, quantifying and predicting soil erosion, most models do not reliably predict erosion yield over large heterogeneous areas (Trimble and Crosson, 2000). The most prominent reasons for this lack of reliability are: (1) insufficient input data with high spatial and temporal resolution (De Jong, 1994); (2) inefficient calibration (Folly et al., 1999); and (3) uncertainty associated with model parameters (De Roo, 1998). Moreover, few erosion models have been developed to continuously simulate the erosion process over long periods, mainly because they do not include temporally dynamic variables such as vegetation growth and groundwater dynamics (Jetten et al., 1999).

In recent years, a variety of models that address some of the problems described above have been published. For example, SEDEM (Van Rompaey et al., 2001) uses the empirical RUSLE as a simple erosion rate platform in a spatially distributed model and is intended to address low-detail distributed data in large catchments. Despite its simplicity, the model accurately calculates sediment delivery, but the empirical RUSLE requires intensive calibration.

Temporally dynamic erosion calculation has been addressed by a variety of landscape evolution models, such as SIBERIA (Willgoose et al., 1991), GOLEM (Tucker and Slingerland, 1994), LAPUS (Schoorl et al., 2000), CHILD (Tucker et al., 2001) and CAESAR (Coulthard et al., 2002). Such landscape evolution models successfully simulate the spatial and temporal distribution of sediment, but are usually complicated to operate and analyze; moreover, detailed input data and outstandingly powerful computers are required.

To address some of the problems associated with conventional modelling, several erosion models have made use of artificial intelligence (AI) technologies (Mitra et al., 1998; Ahamed et al., 2000; Tran et al., 2002). AI has developed rapidly in recent years, providing sophisticated tools to simulate complex environmental processes. Among AI technologies, one of the most promising is the Fuzzy-logic approach (Openshaw and Openshaw, 1997).

Fuzzy-logic has proven to be a useful approach for addressing problems associated with simulating complex processes and environments in a variety of earth science disciplines (Zhu et al., 1996; Tayfur and Singh, 2006; Svoray et al., 2007). The prime advantages of fuzzy-logic are its ability to represent and process uncertain data in the form of moderately continuous classes (Metternicht, 2001); to efficiently model processes with indeterminate boundaries (Burrough, 1996); and to facilitate more flexible knowledge-based modelling developments (Tran et al., 2002). These capabilities enable fuzzy-logic to deal with imprecise and uncertain data and relationships (Mitra et al., 1998), allowing modellers to reduce inherent dependencies on empirical features when designing a model.

In soil sciences, fuzzy-logic is traditionally used to improve the spatial classification of various soil features, such as soil stability (Burrough et al., 1992). Soil erosion modelling has also been addressed with fuzzy-logic in a variety of procedures and to various degrees. Some studies have used the proven ability of fuzzy-logic in spatial classification of soils to improve the spatial characteristics of a given model, such as the USLE (Ahamed et al., 2000). Others have modified a model (e.g. the RUSLE) to fit the fuzzy-logic approach (Tran et al., 2002), thereby improving its performance and overcoming issues of uncertainty, while increasing model flexibility and realistic description of the relationships between its parameters. Fuzzy-logic algorithms have been successfully employed in several hydrological watershed management studies (Tayfur et al., 2003). They have also been used for designing a simple catchment-scale soil erosion model (Mitra et al., 1998) which has proved to be useful in applications with low quality inputs. Most of the related studies have indicated that fuzzy-logic is a flexible and easy-to-apply approach, a vital benefit for both modelers and end-users.

The need for further improvement of fuzzy-logic-based erosion modelling is noted in many publications. The advantage of using fuzzy-logic for erosion modelling was suggested in the discussion of the MEDRUSH, physically-based, catchment-scale model (Kirkby and McMahon, 1999). More relevant, a simple fuzzy-logic sediment transport model was compared to a physically-based model; the results demonstrate the superiority of the latter, showing that fuzzy-logic, despite its various advantages, cannot replace a physically-based model (Tayfur et al., 2003). Therefore, a need arises for the development of a more physically-based fuzzy-logic model.

To address these issues, we have designed a simple and easy to apply catchment-scale soil erosion model, based on physical principles. The model, named FuDSEM (fuzzy-based dynamic soil erosion model) has been designed to assist catchment management and planning. This has been achieved by: (1) simulating soil erosion processes utilizing known principles; (2) using a fuzzy-logic structure to reduce calibration requirements and simplify the output analysis; and (3) using accessible input data, thus minimizing pre-processing.

FuDSEM runoff and erosion predictions were validated in a small data-rich catchment, before implementation in a medium-scale and heterogeneous catchment. The medium-scale predictions were examined by: (1) comparing the runoff component to measured channels flows and (2) comparing the model's erosion predictions against those of two other erosion models in a well-surveyed area.

Modelling approach

Model framework

Fuzzy-logic is a theory in formal mathematics that enables a definitive solution to be obtained for problems that are complex, uncertain and unstructured (Bojorquez-Tapia et al., 2002). A general fuzzy system is composed of three primary elements: fuzzy sets, membership functions (MFs) and fuzzy production rules. A fuzzy set (A) may be defined as follows (Burrough et al., 1992):

For each $A = \{x, \mu_A(x)\} \quad x \in X \quad (1)$

where $X = \{x\}$ is a finite set of points and $\mu_A(x)$ is a membership function of x in A .

The membership function describes the variable's membership assigned to A and, therefore, it may quantify the influence of the variable x on the predicted phenomenon, as it is grasped by the developer (Burrough and McDonnell, 2000). To integrate the effects of a number of variables, several membership functions can be merged in a variety of joint membership functions (JMF). Both membership and joint membership functions provide a simple membership grade in a range of 0–1, where 1 is full membership and 0 is no membership. Here, we use the term 'potential' to describe this mathematical grade, using more process-related terminology. For example, runoff potential means that the membership grade has a high possibility of runoff development.

In general, FuDSEM predicts the hillslope soil erosion potential for each day that exceeds a user-defined precipitation depth value in a meteorological database. It is based

on the infiltration excess runoff mechanism (Hortonian) on hillslopes, with emphasis on the temporal dynamics of this process. FuDSEM divides the erosion process into a sequence of four sub-routines including (Fig. 1): (1) antecedent conditions of soil moisture; (2) runoff generation; (3) transport capacity; and (4) soil erosion. Using fuzzy-logic, each sub-routine is calculated by an individual JMF that combines the relevant parameters (represented by membership functions).

FuDSEM is executed as follows:

- (1) Soil moisture potential (JMF1) is explicitly calculated.
- (2) Runoff potential (JMF2) is calculated by considering the soil moisture potential.
- (3) Runoff potential is spatially accumulated, based on digital elevation model (DEM) data.
- (4) Runoff transport capacity potential (JMF3) is calculated, based on the accumulated and in situ runoff potential.

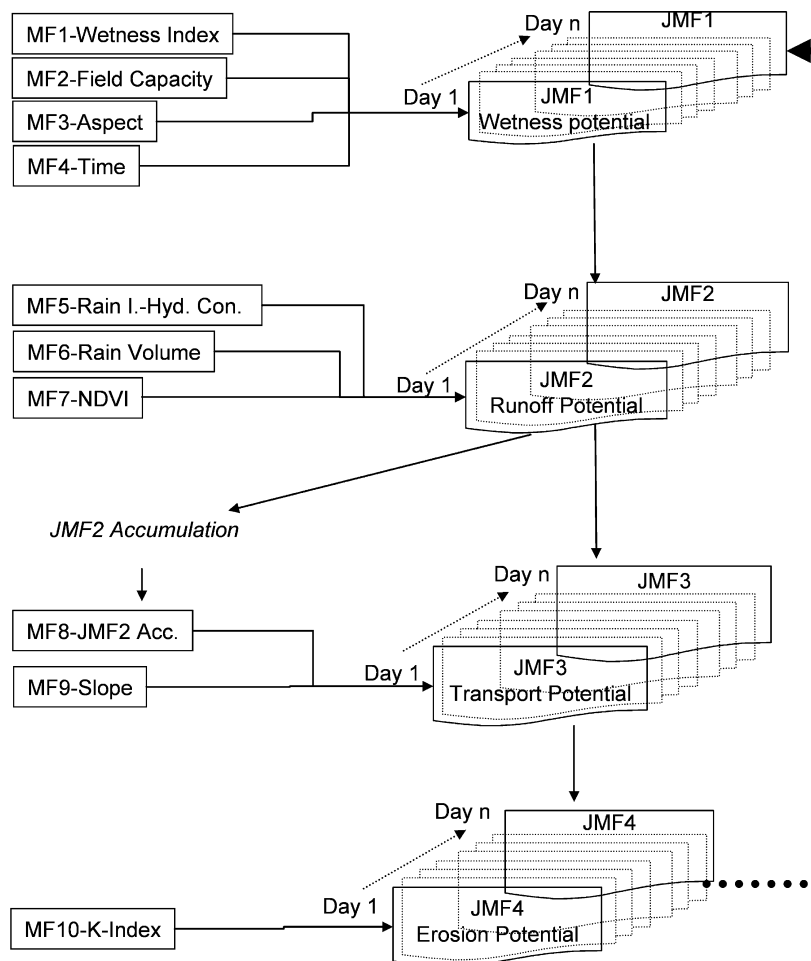


Figure 1 FuDSEM flow chart. FuDSEM operates in daily intervals divided into four sub-routines, each calculated by a distinct JMF. All model parameters are represented in membership functions, converting their values into a membership score assigned to the relevant set. JMF1 represents the cell soil moisture potential that acts as input parameter in JMF2, the cell runoff potential. The cell runoff potential is spatially accumulated, based on a flow direction layer. The original and accumulated runoff potential acts as input parameters in JMF3 calculation, the runoff sediment transport capacity. JMF3 acts as an input parameter in the final sub-routine, the calculation of a cell's erosion potential (JMF4). After producing the erosion potential map, FuDSEM advances to the next day on the database and recalculates the four sub-routines with the new values.

- (5) Soil erosion potential (JMF4) is calculated, based on the transport capacity potential.
- (6) The model proceeds to the next day in the meteorological database, until we reach the last day in the wet season.

These sub-routines are detailed in the following sections.

The functions and weights used in FuDSEM are the outcome of generalized interpretation of common knowledge of erosion processes. Unlike standard, physically-based models, the weights are not intended to represent an accurate quantitative relationship between the parameters, but to provide a general interpretation of the process, as envisaged by the modeller (Baja et al. 2002; Robinson 2003). This is acceptable, since the model predicts the potential of the parameters, thus representing its relative spatial and temporal distribution, rather than providing a quantitative prediction of erosion yield. Therefore, the relationships between the parameters (i.e. functions and weights) are not directly linked to a specific study, but were chosen through a combination of information taken from the relevant literature and expert knowledge.

Soil moisture potential (JMF1)

Antecedent soil moisture conditions are an important parameter in runoff generation. They may vary considerably over time (Jetten et al., 1999), especially in semi-arid environments characterized by scattered rainfall events. FuDSEM estimates soil moisture conditions by linking four parameters: (1) time elapsed from the previous rainfall event (Te); (2) wetness index (WI; Barling et al., 1994); (3) hillslope aspect (SA); and (4) soil field capacity (FC). The membership functions assigned to the parameters in this sub-routine represent the membership score for the high soil moisture conditions set (A_1). The membership score of Te assigned to A_1 is calculated, using the 'left shoulder sigmoidal' membership function (Robinson, 2003; Fig. 2d) generally described by

$$\mu A_i = \frac{1}{1 + e^{\beta(x-\alpha)}} \quad (2)$$

where α is the mid membership value of x and β is the function slope. The left shoulder sigmoidal function was chosen on the basis of the exponential ratio in soil moisture decrease with time (Hillel, 1998). The function parameters

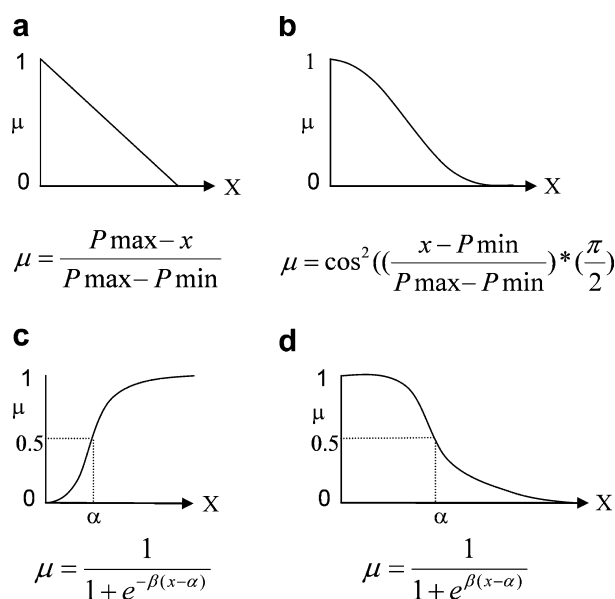


Figure 2 Schematics of four membership functions used in FuDSEM: (a) linear (Robinson, 2003); (b) sigmoidal (Urbanski, 1999); (c) left shoulder sigmoidal (Robinson, 2003); and (d) right shoulder sigmoidal (Robinson, 2003).

(α and β listed in Table 1), were estimated, based on expert knowledge.

The hillslope aspect represents the influence of solar radiation flux on soil moisture as a function of aspect azimuth. In the northern hemisphere, south-facing slopes are commonly less humid, due to higher solar exposure (Oliphant et al., 2003). Therefore, the SA membership score assigned to A_1 increases as a function of radial distance from a 180° aspect azimuth. Based on Svoray et al. (2004), the membership score of SA assigned to A_1 was calculated using a sigmoidal membership function (Urbanski, 1999; Fig. 2b) generally described by the following equation:

$$\mu A_i = \cos^2 \left(\frac{(x - P_{\min})}{(P_{\max} - P_{\min})} \frac{\pi}{2} \right) \quad (3)$$

where x is the input value and P_{\max} and P_{\min} are the maximum and minimum values of the variable x . The function's parameters (P_{\max} and P_{\min}), listed in Table 1, are based on the values reported in Svoray et al. (2004).

Table 1 Summary of FuDSEM parameters, membership function types and membership function coefficients

JMF	Factor	Membership function type	α	β	P_{\min}	P_{\max}
1.	Wetness index	Sigmoidal			0	0.32
	Aspect	Sigmoidal			0	360
	Field capacity	Linear			6.1	42
	Time	Left shoulder	2	1		
2.	Infiltration Excess	Sigmoidal			0	2000
	Rain depth	Sigmoidal			0	40
	NDVI	Linear			0	0.95
3.	Accumulation	Linear			0	10
	Slope	Right shoulder	30	0.1		
4.	K -index	Linear			0.33	0.52

The wetness index is a widely used equation, based on division of the cell slope by its contributing area

$$WI_i = Ln \left[\frac{As_i}{\tan \beta_i} \right] \quad (4)$$

where As is the upper drainage area of a given cell (i) in m^2 and β represents the gradient of the cell in degrees (Barling et al., 1994). Natural logarithms are used to avoid the large numbers that may be produced in large drainage areas. High WI values indicate a higher membership score assigned to the set A_1 . The WI membership score assigned to A_1 is calculated by a mirror version of the sigmoidal membership function (Urbanski, 1999), generally described by Eq. (5)

$$\mu_{A_1} = \cos^2 \left(\frac{(x - P_{\max}) \pi}{(P_{\max} - P_{\min}) 2} \right) \quad (5)$$

The function parameters (P_{\max} and P_{\min}), listed in Table 1, are based on the values reported in Svoray et al. (2004).

The effect of soil characteristics on soil moisture is represented by the field capacity of the soil in each cell. The water holding capacity of the soil varies considerably with soil texture, organic matter content and other physical characteristics (Hillel, 1998). Thus, high FC values increase the cell membership assigned to the set A_1 . Based on De Jong (1994) and Svoray et al. (2004) the membership score is described by a mirror version of the linear membership function (Robinson, 2003; Fig. 2a) generally described by the following equation:

$$\mu_{A_1} = - \frac{P_{\min} - x}{P_{\max} - P_{\min}} \quad (6)$$

The function parameters (P_{\max} and P_{\min}) are simply the maximum and minimum values of the database.

The JMF, combining the soil moisture potential parameters, is formulated with the 'No Trade Off' (NTO) convex combination JMF (Urbanski, 1999) generally described by

$$JMF = \left(\sum_{j=1}^m \lambda_j \mu_{A_j} \right) \wedge \left(\sum_{j=1}^n \lambda_j \mu_{A_j} \right) \quad (7)$$

where $\lambda_{1, \dots, n}$ are the weights of the membership functions and \wedge is the minimum between the two groups of membership functions. This operator was chosen on the assumption that if sufficient time has passed since the last rainfall event, the top soil will dry out regardless of any other parameters. Under these conditions, the dominant parameter influencing the soil moisture potential is Te ; thus, if $Te = 0$, then $JMF1 = 0$. The weight assigned to Te in the JMF is double that of the other parameters, due to its important role in the moisture loss process in semi-arid regions. All the other parameters were assigned an equal weight, under an assumption of equal contribution to the soil moisture potential. The final soil moisture potential JMF is presented in the following equation:

$$JMF1 = \begin{cases} 0.0 & Te = 0 \\ 0.4Te + 0.2SA + 0.2FC + 0.2WI & Te > 0 \end{cases} \quad (8)$$

Runoff potential (JMF2)

The daily runoff potential is simulated only in cells with infiltration excess. Cells with no excess infiltration are assigned a zero runoff potential. Calculating the runoff poten-

tial for a cell with excess infiltration is undertaken by joining four parameters: (1) soil moisture potential (JMF1); (2) excess infiltration (IE); (3) daily rainfall depth (RD); and (4) vegetation cover (NDVI – normalized difference vegetation index; Tucker, 1979).

The membership functions assigned to the parameters in this sub-routine represent the membership score of the set of highest runoff generation potential (A_2). The value of JMF1 represents the cell membership assigned to A_2 , under the assumption that high soil moisture content increases the possibility for runoff generation.

Excess infiltration is calculated by subtracting the saturated hydraulic conductivity of the soil from the daily rainfall intensity. The mirror version sigmoidal membership function (Urbanski, 1999; Eq. (5)) is used to convert the excess infiltration values into the membership score assigned to A_2 , based on the relationship described in Moody and Martin (2001) and Valmis et al. (2005). The function parameters (P_{\max} and P_{\min}), listed in Table 1, are simply the maximum and minimum values of the database.

Based on the relationship reported in USDA-SCS (1985), the membership score of daily rainfall depth of A_2 is described by the mirror version sigmoidal membership function (Urbanski, 1999; Eq. (5)).

Vegetation cover affects runoff generation by decreasing raindrop energy and increasing its infiltration rate (Yair and Kossovsky, 2002; Calvo-Cases et al., 2003). Vegetation cover in semi-arid regions is characterized by patchy and heterogeneous distribution, creating a high spatio-temporal variability in water redistribution along the hillslopes (Svoray and Shoshany, 2004). Based on FAO (1967), the membership score of NDVI assigned to A_2 is calculated by a linear membership function (Robinson, 2003; Fig. 2a), which is generally described by the following equation:

$$\mu_{A_1} = \frac{P_{\max} - x}{P_{\max} - P_{\min}} \quad (9)$$

Combining the four membership functions, the calculation of the overall runoff potential is carried out with the NTO JMF (Urbanski, 1999; Eq. (7)), in order to introduce IE as a threshold parameter. As mentioned above, negative or zero IE values yield zero runoff potential. The weight assigned to NDVI is double the weight assigned to the other parameters due to its importance in semi-arid environments (Yair and Kossovsky, 2002). All other parameters were assigned an equal weight under the assumption of equal contribution to runoff potential. The final runoff potential JMF2 is presented in the following equation:

$$JMF2 = \begin{cases} 0.0 & IE \leq 0 \\ 0.2IE + 0.2RD + 0.4NDVI + 0.2JMF1 & IE > 0 \end{cases} \quad (10)$$

Transport capacity potential (JMF3)

The ability of runoff to transport sediments is influenced by a variety of parameters, among them shear stress, vegetation cover and soil and topographic characteristics (Thornes, 1980). The initiation of erosion and transport of sediment by water is performed on hillslopes by unconcentrated runoff and by rill flow. Further downstream, it occurs in and forms gullies and channels. No distinction is made between these in our FuDSEM model, which is acceptable in

non-mechanistic models (Hillel, 1998). Three parameters are linked to calculate the runoff transport capacity potential in the model: (1) runoff potential (JMF2); (2) runoff accumulation (Acc); and (3) local slope decline (S). The membership functions assigned to the parameters in this sub-routine represent the membership score assigned to the set with the highest runoff transport capacity potential (A_3). Runoff potential (JMF2) represents the cell membership score of A_3 , under the assumption that a high value of runoff increases cell transport capacity.

Runoff volume and transport capacity in a given cell are influenced by the runoff generated in situ and by runoff accumulated from its upslope contributing area. Accumulation to a given cell (Acc) is influenced, not only by the contributing area, but also by land cover characteristics of the accumulating catchment. A cell with high runoff potential is regarded as a source for the down-slope cells, while, by contrast, a cell with low runoff potential is considered a sink. Therefore, the runoff accumulation procedure is important for describing the spatio-temporal dynamics of runoff flow. The Acc membership function assigned to A_3 is described by the mirror linear function (Robinson, 2003; Eq. (6)).

Slope represents the effect of gravitational force on runoff discharge. A steep slope increases runoff discharge, resulting in a higher transport capacity. Based on De Jong et al. (1999), we used the 'right shoulder sigmoidal' membership function (Robinson, 2003; Fig. 2c) to describe the membership score of slope of A_3 , as follows:

$$\mu_{A_i} = \frac{1}{1 + e^{-\beta(x-\alpha)}} \quad (11)$$

The parameters α and β (Table 1) were evaluated from the results of a small pan experiment (Kirkby, 1980). Combining the three membership functions to calculate the transport capacity potential is undertaken with the 'convex combination operation function' (Burrough et al., 1992), which is generally described by

$$JMF = \lambda_1 \mu_{A_i} + \lambda_2 \mu_{A_j} + \dots + \lambda_n \mu_{A_k} \quad (12)$$

The three parameters were assigned equal weights in the final transport capacity potential JMF, under an assumption of equal contributions to the process

$$JMF3 = 0.33S + 0.33Acc + 0.33JMF2 \quad (13)$$

Soil erosion potential (JMF4)

The final sub-routine calculates the erosion potential by assuming that in a specific transport capacity, the entrainment of sediments is a function of topsoil erodibility: sediment entrainment and thus, erosion, are expected to increase in more erodible soils. Therefore, the daily erosion potential is calculated by linking the runoff transport capacity (JMF3) with K , the soil erodibility index (Wischmeier and Smith, 1978).

The membership functions assigned to the parameters in this sub-routine represent the membership score to the highest erosion potential set (A_4). JMF3 represents the effect of high transport capacity on the overall erosion potential and K represents topsoil sensitivity to erosion. A high value of erodibility results in higher erosion potential for given runoff conditions. The membership score of K , assigned

to A_4 , is described by the mirror version linear membership function (Robinson, 2003; Eq. (6)), based on Mitra et al. (1998).

Combining the two membership functions to calculate the erosion potential is undertaken with the 'convex combination operation function' (Burrough et al., 1992; Eq. (12)). We assume that the transport capacity potential dominates the final erosion calculation, so we assign it a considerably higher weight than K . The erosion potential JMF is represented by

$$JMF4 = 0.1K + 0.9JMF3 \quad (14)$$

Data used

The Bikhra Catchment

Initial model validation was conducted on the small, data-rich Bikhra Catchment (0.7 km²; Fig. 3) on the southern flanks of the Hebron anticlinorium in central Israel. It is located between a region of Mediterranean climate to the west and north and the aridity of the Judean Desert to the east and of the Negev to the south. Topographically, this area is characterized by round limestone hillocks separated by loess-clad valleys. Loess also covers most of the lower hillslopes. The average annual rainfall is 240 mm, with considerable temporal variation (the coefficient of variation for most rain stations is larger than unity). Rainstorms may either be frontal or convective: the convective storms are spotty in nature (Sharon, 1972), occur most commonly in spring and autumn, and may have very high intensities, such as 200 mm/h for durations of 10–15 min (Sharon and Kutiel, 1986). The frontal, Mediterranean-derived cyclones are typically winter events of longer duration and lower intensities. The soils covering the higher hillslopes are brown lithosols. Colluvium has developed to a limy, stony sierozem at the bottom of some hillslopes. Valley bottoms are loessial, increasing in depth downvalley. Land use includes grazing and overgrazing.

Suspended sediment concentrations were obtained from a pre-programmed automatic 24-bottle water sampler (ISCO) located at the crump weirs. The samplers are activated when flow occurs. Rating curves were derived separately for rising and falling limbs of flow events and suspended sediment yield for each event was calculated. Although bedload fluxes are very high in semiarid environments, more than 92% of the sediment transported by flow events is suspended (Powell et al., 1996). Accordingly and taking into consideration the fact that the proposed model mostly deals with sediment potential supply from hillslopes, we used suspended sediment yield as a proxy for the total yield.

The Shiqma Catchment

The Shiqma Catchment (785 km² in size) is located in central Israel (Fig. 3). The climate is semi-arid, characterized by 350 mm/yr mean annual rainfall, mostly occurring in winter, between October and May (Goldreich, 1998). Rainfall events in this area are typically short, with an average of 40 rainfall days per year. The storm regime is usually frontal

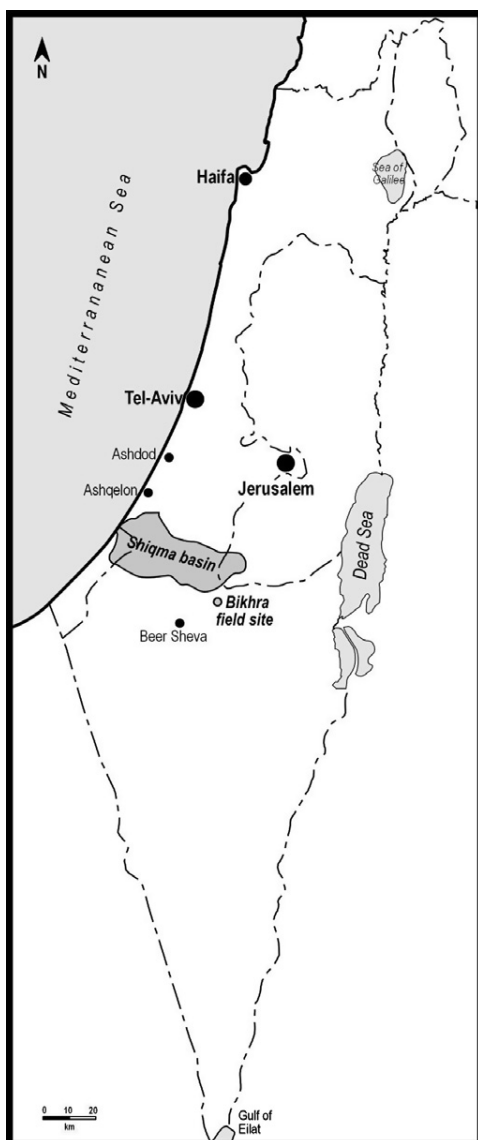


Figure 3 Study site: The Shiqma Catchment (785 km²) and the Bikhra Catchment (0.7 km²).

and extremely variable, with relatively low intensities (FAO, 1967). The semi-natural vegetation of the catchment is mainly natural grassland with scattered trees, shrubs and dwarf shrubs (Shoshany and Svoray, 2002). The catchment's principal land use is agriculture, mainly wheat fields, as well as some fruit plantations. A major source of sediments in the Shiqma Catchment is channel and gully erosion, primarily headwall gully retreat and channel incision (Seginer, 1966; Nir and Klein, 1974; Rozin and Schick, 1996).

Rainfall data

In the Bikhra study, rain gauge data from two consecutive years (2002–2003) were used. Since it is a small catchment, we assume spatial homogeneity. For the Shiqma Catchment, daily rainfall data for three consecutive years (1995–1998) were used. This database was obtained from

eight meteorological stations of the Israel Meteorological Service, consisting of rainfall depth and maximum intensity for a 30 min period for each rainy day. To represent the spatial distribution of rainfall, the study area was divided into eight regions, each represented by a single meteorological station. We used Thiessen polygons for the spatial distribution of rainfall data, instead of the more commonly used interpolation techniques (which are extremely labour intensive for temporally explicit simulations), since our simulation was based on a detailed rainfall database for the entire catchment area.

Soil data

For the Bikhra study site, field capacity and saturated hydraulic conductivity were calculated by averaging four soil samples. For the Shiqma site, average texture data for each soil unit were estimated on the basis of the relevant literature (FAO, 1967; Dan, 1968; Ravikovitch, 1992). Based on soil texture, we calculated the two physical soil characteristics used by FuDSEM: field capacity and saturated hydraulic conductivity using the water soil characteristics software (Saxton, 2005). The USLE *K*-index was estimated based on the soil erodibility table (Mitchell and Bubenzner, 1980). A digital soil map (Dan and Raz, 1970) was used to spatially represent soil characteristics at both study sites.

Topographic data

The Hall and Cleave (1988) DEM from the Geological Survey of Israel, with horizontal resolution of 25 × 25 m² and vertical resolution of 10 m, was used to create the slope, aspect and WI layers in both catchments.

Vegetation cover data

NDVI was used to represent the vegetation cover of the study area during the growing season. A series of four Landsat TM satellite images (from the following dates: 10 November 1996, 14 February 1997, 19 April 1997 and 21 May 1997) was used to calculate NDVI values for both catchments. The temporal pattern of the 1996–1997 growing season was used for the entire series of multi-annual simulations, each NDVI layer representing a specific period of the season (for example the November 10 NDVI represents the spatial distribution of vegetation in simulation, between October 1 and December 31). The Landsat images were radiometrically and geometrically corrected using common procedures (Svoray and Shoshany, 2003).

Model evaluation

Evaluating a distributed large scale soil erosion model has long been acknowledged as difficult, primarily due to absence of reliable spatially distributed sediment data (Merriitt et al., 2003). In order to address this issue, we used, as described above, the small data-rich Bikhra catchment as an initial case study, to validate our FuDSEM runoff and erosion predictions. We then implemented the model on the complex Shiqma Catchment and evaluated its predictions by: (1) sensitivity analysis, comparing the FuDSEM

runoff component to daily runoff measurements and (2) examining the FuDSEM erosion predictions in two surveyed sub-catchments.

Small scale correlation analysis (the Bikhra study)

Runoff and suspended sediment load measurements at the Bikhra outlet from 11 rainfall events were used to validate FuDSEM. Runoff predictions were evaluated by calculating the correlation between the average runoff potential (JMF2) of the catchment and the measured runoff. Similarly, the average erosion potential (JMF4) in each event was compared to the measured suspended sediment load at the catchment outlet.

Large scale runoff sensitivity analysis

One of the most commonly used hydrological measurements applicable for large catchments is that of channel flow levels. We used flow level measurements from five hydrological stations across the catchment (Fig. 4) to evaluate the FuDSEM runoff potential predictions (JMF2). The five stations are located in channels draining catchments for a wide range of sizes (16–378 km²). Station flow was compared to average FuDSEM runoff prediction. The correlation between the predicted and measured runoff in each catchment was evaluated and plotted. The outliers of this analysis were utilized to conduct a sensitivity analysis of the FuDSEM runoff component, by examining the model's over- and under-predictions.

Site-specific comparison

Two adjacent sub-catchments with considerable difference in erosive characteristics were identified in a field survey of the central Shiqma Catchment. The eastern sub-catchment

is characterized as erosive, due to deeply incised channels, eminent headwall gully retreat and signs of fresh rilling on the slopes. The western sub-catchment appears to be stable and less erodible, as no signs of recent erosion activity were observed. To validate and quantify this observation, the drainage density evolution was calculated for both sub-catchments. Drainage density evolution was monitored by digitizing the catchments' channel network on three dates of observation (1945, 1970 and 2000), based on aerial photographs and GPS verification. Drainage density was calculated by dividing the overall channel length by the sub-catchment area (Chow et al., 1988). FuDSEM's three year erosion potential predictions were calculated for the two sub-catchments. The differences between model prediction and drainage density were used to evaluate FuDSEM's multi-year erosion prediction for that region.

The FuDSEM predictions were also compared with two erosion models: a temporally static version of FuDSEM (FuSEM – fuzzy-based soil erosion model) and the soil erosion model for Mediterranean regions (SEMMED; De Jong, 1994; De Jong et al., 1999). FuSEM differs from FuDSEM only in that it uses average rainfall values, excludes Ta and uses only one NDVI layer (at mid-season – 14 February 1997) to represent the vegetation cover. FuDSEM and FuSEM were compared to better understand the influence of the temporally dynamic mechanism on multi-annual predictions.

SEMMED is a physically-based semi-empirical model, calibrated for Mediterranean regions. It is based on the MMF (Morgan–Morgan–Finny; Morgan et al., 1984) approach and was modified for regional scale, by using remotely sensed data and GIS techniques (De Jong 1994; De Jong et al., 1999). We used SEMMED as a comparison model, since its input data are generally similar to those used by FuDSEM (remote sensing and GIS data) and the model is designed for Mediterranean regions. By comparing FuDSEM and SEMMED, we hoped to show the benefits of a simple and relative ero-

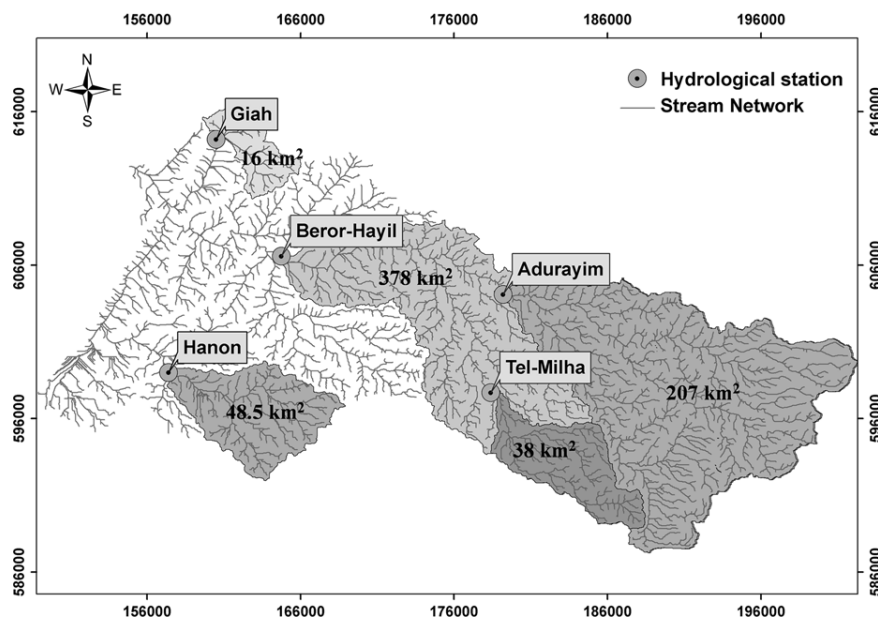


Figure 4 The Shiqma Catchment and the five hydrological stations with their contributing drainage catchments. The numbers in each drainage catchment represent its drainage area.

sion prediction (i.e. FuDSEM) over a standard physically-based soil erosion model.

Results and discussion

Small scale correlation analysis

The FuDSEM runoff potential prediction (JMF2) and erosion potential predictions (final JMF) were regressed against the corresponding measured runoff and sediment load in the Bikhra catchment. The results are shown in Fig. 5a and b, respectively. In this event-based analysis, the measured runoff and sediment data are viewed on a logarithmic scale for comparison with the FuDSEM potential prediction scale. Strong linear correlations are observed in $n = 11$ different events, distributed over two years ($r^2 = 0.79$) in the case of runoff and similarly ($r^2 = 0.76$) in the case of erosion/sediment analysis. These results allow us a considerable degree of confidence in the calibration of both the runoff component (JMF2) and the final prediction of the model. This outcome meant that we could apply FuDSEM to the more complex, medium-scale Shiqma Catchment.

Large scale implementation

Fig. 6a shows FuDSEM's three-year erosion potential map of the Shiqma Catchment, calculated by averaging all predicted daily maps. This map was used to evaluate the spatial

distribution of FuDSEM output and compare it with the FuSEM and SEMMED prediction maps (Fig. 6b and c, respectively).

Distinct differences appear between diverse parts of the Shiqma Catchment (Fig. 6a). The eastern part of the catchment was assigned the highest erosion potential, while the lowest prediction values were scattered in clusters within the center and western regions. These results are affected, to some extent, by the spatial patterns of soil, as reflected in the soil map. However, FuSEM's output (Fig. 6b) neither shows distinct spatial distributions, nor can it be linked to the soil map. Moreover, its output map is considerably noisier and less interpretable at the catchment management level. The SEMMED three-year erosion prediction (Fig. 6c) is fundamentally different from the other two, since its values are quantitative, whereas those of FuDSEM and FuSEM are relative. From a catchment interface point of view, SEMMED provides little knowledge about the spatial distribution of erosion.

This qualitative comparison between the three maps reveals important differences between the three models. From a catchment management standpoint, the continuous representation of erosion (as provided by the fuzzy-based models) seems to be a major advantage, providing a comparison between different parts of the catchment. The scattered distribution produced by SEMMED appears to be less useful for large scale environmental analysis, since identification of variation in erosion within the catchment is more complicated, requiring knowledge and experience in erosion yield quantification and interpretation.

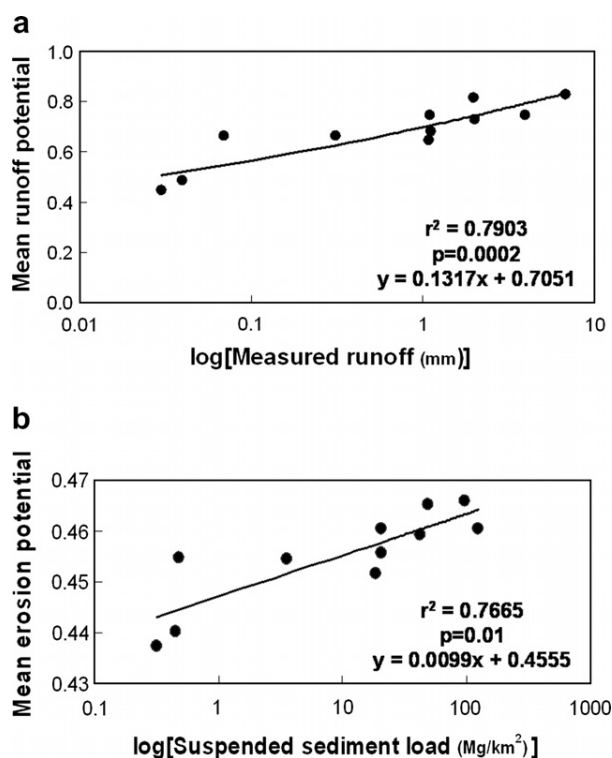


Figure 5 Plots of (a) predicted mean FuDSEM runoff potential versus measured runoff at the outlet of the Bikhra catchment on a logarithmic scale and (b) predicted mean FuDSEM erosion potential versus measured sediment load at the outlet of the Bikhra catchment on a logarithmic scale.

Runoff sensitivity analysis

The correlation plots between predicted and measured runoff in the five hydrological stations are presented in Fig. 7. The coefficients of determination in the three eastern stations (Beror-Hayil, Adorayim and Tel-Milha) are relatively low, while in the western stations (Giah and Hanon), the coefficients are considerably higher. This difference can be attributed to variations in the stations' drainage areas. Generally, stations with a large drainage catchment (Beror-Hayil with 378 km² and Adorayim with 207 km²) have low coefficients of determination, compared to smaller drainage catchments (Giah with 16 km² and Hanon with 48.5 km²). One exception to this finding is the Tel-Milha station – despite its relatively small drainage catchment (38 km²), it has a low coefficient of determination.

These results show a serious drawback in using large and heterogeneous catchments as prime elements for validation. The explanation for this observation is that the empirical outlet data represent the average/generalized value, rather than reliably representing the diversity of conditions in the sub-catchments. Though no rigid conclusions are drawn from the five catchments, we used those stations with a higher correlation (Giah and Hanon) to identify outlier days (i.e. under- and over-estimations). The meteorological properties of the outlier days and the physical properties of the drainage catchments were thereafter examined. Two main factors explain most of the outliers: (1) the excess infiltration simulation in FuDSEM's runoff mechanism leads to several under-predictions. In days with low to moderate rainfall intensity, FuDSEM predicted no runoff generation in cells with high saturated hydraulic

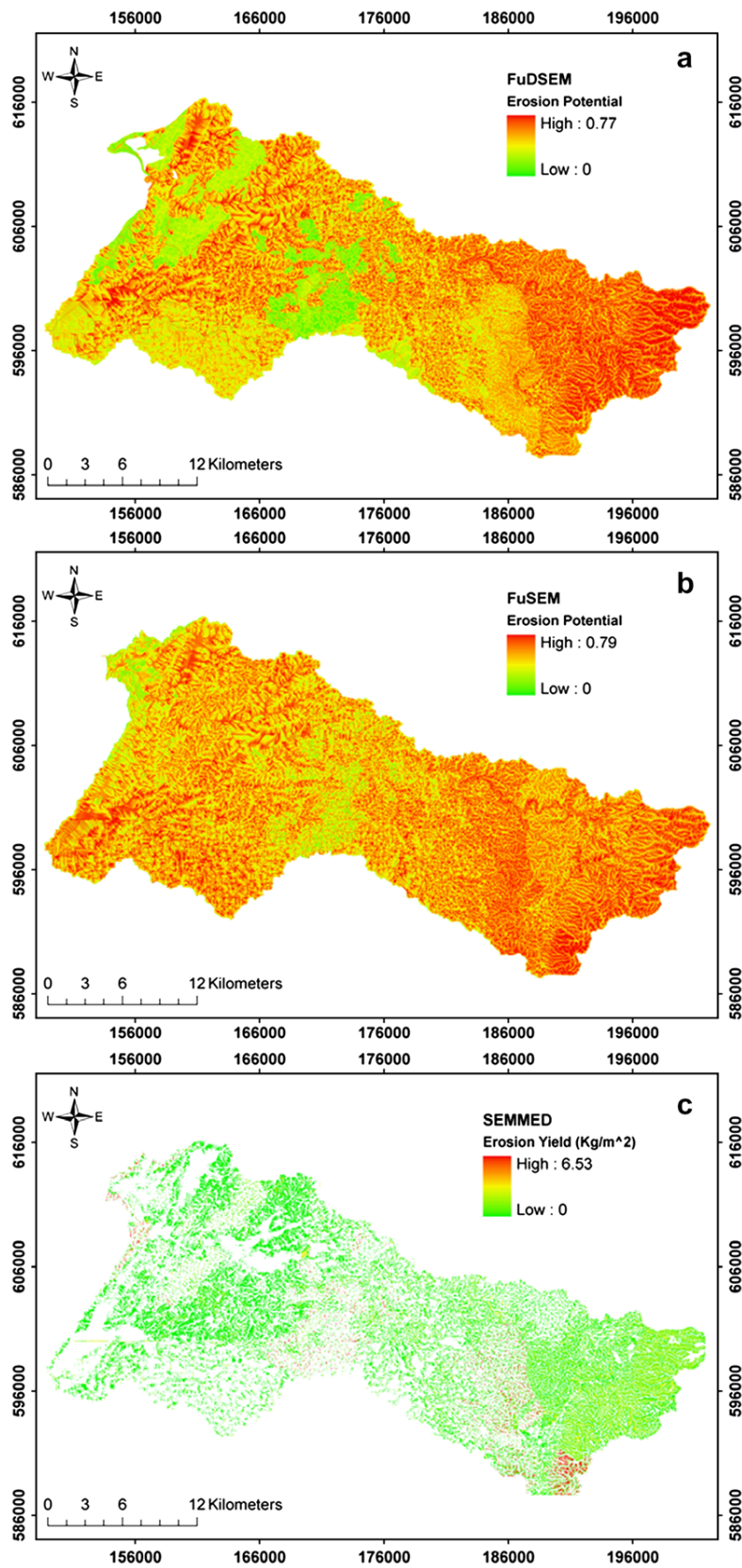


Figure 6 Shiqma Catchment three-year erosion prediction maps of (a) FuDSEM, (b) FuSEM and (c) SEMMED.

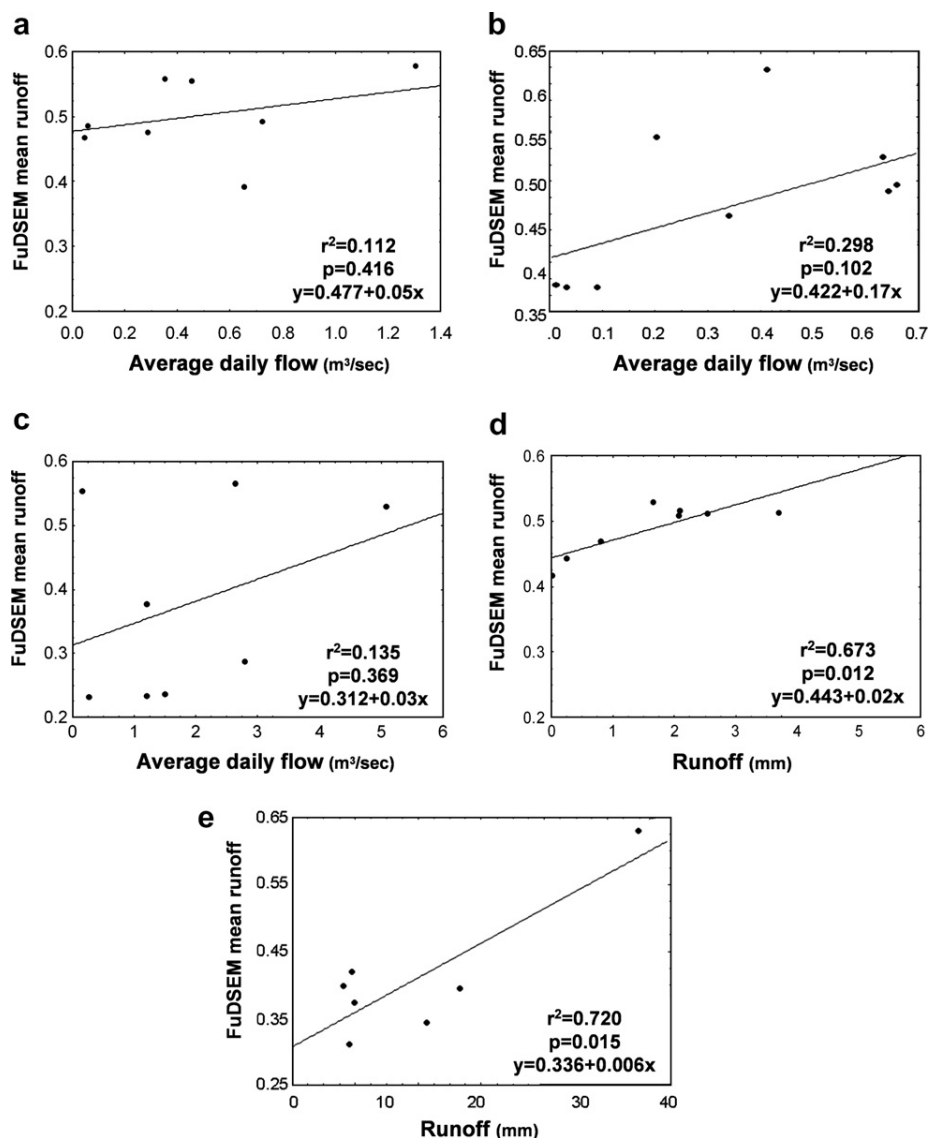


Figure 7 Plots of FuDSEM predicted runoff versus measured runoff at hydrological stations: (a) Adurayim, (b) Beror-Hayil, (c) Tel-Milha, (d) Hanon and (e) Giah.

conductivity values (under the assumption that excess infiltration is the only runoff mechanism in the study area). Apparently, this is not the case in all circumstances. All under-predicted days were part of a continuing rainfall event (i.e. the day preceding them was also rainy). This may indicate that a saturation runoff mechanism may also occur in this area. (2) Rainfall intensity simulation in FuDSEM's runoff mechanism seems to yield lower predictions on those days, which may have led to over-prediction for low intensity rainfall events. Due to the importance of rainfall intensity on runoff mechanism in semi-arid environments, we used it as a conditioning factor in FuDSEM's runoff mechanism (section "Runoff Potential (JMF2)").

Site-specific comparison

The measured drainage density evolution in the two sub-catchments was used to validate and quantify the field sur-

vey observations. Table 2 summarizes those values, which show that the western sub-catchment had a denser drainage network in 1945 and 1970, compared to the eastern sub-catchment (a ratio of 0.76 and 0.69, respectively); the ratio shifted in the next 30 years to 1.54 in 2000. This result corresponds well with the field observation, in which we classified the eastern sub-catchment as presently being more erosive. This result corresponds well with the findings at the nearby Huga sub-catchment, extending over approximately the same time frame (Rozin and Schick, 1996). Rozin and Schick showed that, as a result of reduction in grazing and other agricultural activities (as observed in the western sub-catchment), vegetation growth dramatically reduced erosion and stabilized the channel network.

The average erosion prediction of the three models (FuDSEM, FuSEM and SEMMED), within the two sub-catchment (Table 3), shows that FuDSEM was the only model to predict higher erosion in the eastern sub-catchment, as compared

Table 2 Eastern and western sub-catchments drainage density evolution and drainage density ratio in 1945, 1970 and 2000

	Year		
	1945	1970	2000
<i>Eastern sub-catchment</i>			
Channel length (km)	8.633	6.869	9.947
Catchment area (km ²)	1.476	1.476	1.476
Density	0.006	0.005	0.007
<i>Western sub-catchment</i>			
Channel length (km)	3.844	3.372	2.199
Catchment area (km ²)	0.505	0.505	0.505
Density	0.007	0.006	0.004
Density ratio (eroded/stable)	0.768	0.697	1.547

Table 3 Average three-year prediction of the three models in the eastern and western sub-catchments and the ratio between them

Model	Eastern sub-catchment	Western sub-catchment	Ratio (eastern/western)
FuSEM	0.30	0.33	0.92
FuDSEM	0.20	0.16	1.25
SEMMED	0.02	0.04	0.59

The eastern sub-catchment was characterized as erosive while the western was stable.

to the western sub-catchment. The ratio between the eastern and western sub-catchments, in terms of average erosion prediction by FuDSEM, FuSEM and SEMMED (1.25, 0.92 and 0.59, respectively; Table 3), shows the advantage of FuDSEM over the other two models. These results also show the advantage of FuSEM over SEMMED, indicating the superiority of the fuzzy-based approach. The advantage of FuDSEM over FuSEM clearly demonstrates that a temporally-dynamic structure is a crucial component for model accuracy in fuzzy modelling.

Conclusions

A strong correlation was observed between predicted runoff and erosion potential by the FuDSEM model and measured runoff and erosion/sediment in the small-scale data-rich study of the Bikhra catchment. This finding gives considerable confidence in the model structure, thereby allowing us to proceed to medium-scale implementation in the Shiqma Catchment. However, the comparison between measured and average runoff in five sub-catchments at Shiqma reveals serious drawbacks in large scale runoff analysis. Despite this finding, the outliers of this correlation analysis were used for a simple sensitivity analysis. Overestimation was found for the infiltration excess sub-model (IE) and underestimation in the case of rainfall intensity factor in some rainfall conditions. Nevertheless, the results are significant and these inaccuracies should be studied in future research.

The comparison between the FuDSEM, FuSEM and SEMMED maps shows the advantage of the fuzzy-logic model in representing spatial distribution of erosion. FuDSEM produces more continuous and easy to interpret maps, important attributes for large scale interface management. The site-specific comparison of drainage density between the three models also demonstrates the advantage of FuDSEM, the only model to accurately predict the differences between two surveyed sub-catchments. Keeping in mind the limitation of this method, the findings validate the proposed benefits of FuDSEM's temporally dynamic and fuzzy-logic structure.

Inherently, FuDSEM produces potential, qualitative erosion maps, not quantitative erosion values. The advantages of the qualitative maps for catchment management purposes are: (1) continuous spatial distributions that are easier to interpret at large scales; (2) it may be easily understood by laymen; and (3) it offers a clearer display of erosion hot spots within a catchment. For engineering purposes it is apparent that one of the traditional quantitative erosion models should be utilized to analyse small sites located by FuDSEM.

This work shows the potential of FuDSEM architecture in representing the distribution of erosion possibility. So far, the model has only been initially examined, but it demonstrates the benefits of a fuzzy-logic based approach in a mechanistic erosion model. Although showing considerable potential, further validation and adjustments of FuDSEM are required.

Acknowledgments

This research was funded by the Soil Branch Advisory Board of the Israel Ministry of Agriculture and Rural Development, Program No. 857046802. We thank the Geological Survey of Israel for allowing the use of the DEM; Israel Hydrological Service for providing runoff data; Israel Meteorological Service for providing rainfall data; Survey of Israel for supplying the aerial photographs; the Soil Erosion Research Station and its Head, Shmuel Arbel, for providing runoff and rainfall data. Monitoring at the Bikhra sub-catchment was funded by AID project M20-022. Particular thanks are extended to Ilana Frank-Wener for hard-won sediment and water discharge data and also to Jiftah Ben-Asher and Joel Dan for productive conversations.

References

- Ahamed, T.R.N., Rao, K.G., Murthy, J.S.R., 2000. Fuzzy class membership approach to soil erosion modelling. *Agric. Syst.* 63, 97–110.
- Baja, S., Chapman, D.M., Dragovich, D., 2002. A conceptual model for defining and assessing land management units using a fuzzy modeling approach in GIS environment. *Environ. Manage.* 29, 647–661.
- Barling, R.D., Moore, I.D., Grayson, R.B., 1994. A quasi-dynamic wetness index for characterizing the spatial-distribution of zones of surface saturation and soil-water content. *Water Resour. Res.* 30, 1029–1044.
- Bojorquez-Tapia, L.A., Juarez, L., Cruz-Bello, G., 2002. Integrating fuzzy logic, optimization, and GIS for ecological impact assessments. *Environ. Manage.* 30, 418–433.

- Burrough, P.A., 1996. Natural objects with indeterminate boundaries. In: Burrough, P.A., Franck, A.U. (Eds.), *Geographic Objects with Indeterminate Boundaries*. Taylor and Francis, London.
- Burrough, P.A., Macmillan, R.A., Vandeursen, W., 1992. Fuzzy classification methods for determining land suitability from soil-profile observations and topography. *J. Soil Sci.* 43, 193–210.
- Burrough, P.A., McDonnell, R.A., 2000. *Principles of Geographical Information Systems*. Oxford University Press, New York.
- Calvo-Cases, A., Boix-Fayos, C., Imeson, A.C., 2003. Runoff generation, sediment movement and soil water behavior on calcareous (limestone) slopes of some Mediterranean environments in southeast Spain. *Geomorphology* 50, 269–291.
- Chow, V.T., Maidment, D.R., Mays, L.W., 1988. *Applied Hydrology*. McGraw-Hill, New York.
- Coulthard, T.J., Macklin, M.G., Kirkby, M.J., 2002. A cellular model of Holocene upland river basin and alluvial fan evolution. *Earth Surf. Proc. Land.* 27, 269–288.
- Dan, J., 1968. *A Key for the Soils of Israel*. The Volcani Center, Beit-Dagan, Israel (in Hebrew).
- Dan, J., Raz, Z., 1970. *The Soil Formation Map of Israel*. The Volcani Center, Beit-Dagan, Israel (in Hebrew).
- De Jong, S.M., 1994. *Application of Reflective Remote Sensing of Land Degradation Studies in a Mediterranean Environment*. Netherlands Geographical Studies, Utrecht.
- De Jong, S.M., Paracchini, M.L., Bertolo, F., Folving, S., Megier, J., de Roo, A.P.J., 1999. Regional assessment of soil erosion using the distributed model SEMMED and remotely sensed data. *Catena* 37, 291–308.
- De Roo, A.P.J., 1998. Modelling runoff and sediment transport in catchments using GIS. *Hydrol. Process.* 12, 905–922.
- De Roo, A.P.J., Wesseling, C.G., Ritsema, C.J., 1996. LISEM: a single-event physically based hydrological and soil erosion model for drainage catchment. 1. Theory, input and output. *Hydrol. Process.* 10, 1107–1117.
- Food and Agriculture Organization of the United Nations (FAO), 1967. *Pilot Project in Watershed Management on Nahal Shikma*. United Nations Development Program, Rome.
- Folly, A., Quinton, J.N., Smith, R.E., 1999. Evaluation of the EUROSEM model using data from the Catsop watershed, The Netherlands. *Catena* 37, 507–519.
- Goldreich, Y., 1998. *The Climate of Israel: Observations, Research and Applications*. Bar-Ilan University Press, Ramat-Gan (in Hebrew).
- Hall, J.K., Cleave, R.L., 1988. The DTM project. *Geol. Surv. Israel* 6, 1–7.
- Hillel, D., 1998. *Environmental Soil Physics*. Academic Press, New York.
- Jetten, V., de Roo, A., Favis-Mortlock, D., 1999. Evaluation of field-scale and catchment-scale soil erosion models. *Catena* 37, 521–541.
- Jetten, V., Govers, G., Hessel, R., 2003. Erosion models: quality of spatial predictions. *Hydrol. Process.* 17, 887–900.
- Kirkby, M.J., 1980. Modelling water erosion processes. In: Kirkby, M.J., Morgan, R.P.C. (Eds.), *Soil Erosion*. John Wiley & Sons, New York, pp. 183–216.
- Kirkby, M.J., McMahon, M.L., 1999. MEDRUSH and the Catsop Catchment – the lessons learned. *Catena* 37, 495–506.
- Merritt, W.S., Letcher, R.A., Jakeman, A.J., 2003. A review of erosion and sediment transport models. *Environ. Modell. Software* 18, 761–799.
- Metternicht, G., 2001. Assessing temporal and spatial changes of salinity using fuzzy logic, remote sensing and GIS, foundations of an expert system. *Ecol. Modell.* 144, 163–179.
- Mitchell, J.K., Bubenzer, G.D., 1980. Soil loss estimation. In: Kirkby, M.J., Morgan, R.P.C. (Eds.), *Soil Erosion*. John Wiley & Sons, New York, pp. 17–62.
- Mitra, B., Scott, H.D., Dixon, J.C., McKimmey, J.M., 1998. Applications of fuzzy logic to the prediction of soil erosion in a large watershed. *Geoderma* 86, 183–209.
- Moody, J.A., Martin, D.A., 2001. Post-fire, rainfall intensity-peak discharge relations for three mountainous watersheds in the western USA. *Hydrol. Process.* 15, 2981–2993.
- Morgan, R.P.C., Morgan, D.D.V., Finney, H.J., 1984. A predictive model for the assessment of soil-erosion risk. *J. Agric. Eng. Res.* 30, 245–253.
- Morgan, R.P.C., Quinton, J.N., Rickson, R.J., 1992. *EUROSEM Documentation Manual*. Version 1, June 1992. Silsoe College, Silsoe.
- Nir, D., Klein, M., 1974. Gully erosion induced by changes in land use in a semiarid terrain (Nahal Shiqma, Israel). *Zeitschrift für Geomorphologie, Supplementband* 21, 191–201.
- Nearing, M.A., Foster, G.R., Lane, L.J., Finkner, S.C., 1989. A process-based soil-erosion model for USDA-water erosion prediction project technology. *Trans. Am. Soc. Agric. Eng.* 32, 1587–1593.
- Oliphant, A.J., Spronken-Smith, R.A., Sturman, A.P., Owens, I.F., 2003. Spatial variability of surface radiation fluxes in mountainous terrain. *J. Appl. Meteorol.* 42, 113–128.
- Openshaw, S., Openshaw, C., 1997. *Artificial Intelligence in Geography*. John Wiley & Sons, West Sussex, p. 329.
- Powell, M.D., Reid, I., Laronne, J.B., Frostick, L.E., 1996. Bedload as a component of sediment yield from a semiarid watershed of the northern Negev. *Int. Assoc. Hydrol. Sci. Publ.* 236, 389–397.
- Ravikovitch, S., 1992. *The Soils of Israel: Formation Nature and Properties*. Hakibbutz Hameuchad, Tel-Aviv (in Hebrew).
- Robinson, V.B., 2003. A perspective on the fundamentals of fuzzy sets and their use in geographic information systems. *Trans. GIS* 7, 3–30.
- Rozin, U., Schick, A.P., 1996. Land use change, conservation measures and stream channel response in the Mediterranean/semiarid transition zone: Nahal Hoga, southern Coastal Plain, Israel. In: *Erosion and Sediment Yield: Global and Regional Perspectives*. Int. Assoc. Hydrol. Sci. Publ. 236, 427–444.
- Saxton, K.E., 2005. PAW: Soil, Plant, Atmosphere, Water Field & Pond Hydrology. Agricultural Research Service, United States Department of Agriculture (USDA), Pullman. <<http://hydro-lab.arsusda.gov/SPAW/Index.htm>>.
- Schmidt, J., Von Werner, M., Michael, A., 1999. Application of the EROSION 3D model to the Catsop watershed, The Netherlands. *Catena* 37, 449–456.
- Schoorl, J.M., Sonneveld, M.P.W., Veldkamp, A., 2000. Three-dimensional landscape process modelling: the effect of DEM resolution. *Earth Surf. Proc. Land.* 25, 1025–1034.
- Seginer, I., 1966. Gully development and sediment yield. *J. Hydrol.* 4, 236–253.
- Sharon, D., 1972. The spotiness of rainfall in a desert area. *J. Hydrol.* 17, 161–175.
- Sharon, D., Kutiel, H., 1986. The distribution of rainfall intensity in Israel, its regional and seasonal variations and its climatological evaluation. *J. Climatol.* 6, 277–291.
- Shoshany, M., Svoray, T., 2002. Multidate adaptive unmixing and its application to analysis of ecosystem transitions along a climatic gradient. *Rem. Sens. Environ.* 82, 5–20.
- Svoray, T., Mazor, S., Bar, P., 2007. How is shrub cover related to soil moisture and patch geometry in the fragmented landscape of the Northern Negev desert? *Landsc. Ecol.* 22, 105–116.
- Svoray, T., Gancharski, S.B.Y., Henkin, Z., Gutman, M., 2004. Assessment of herbaceous plant habitats in water-constrained environments: predicting indirect effects with fuzzy logic. *Ecol. Modell.* 180, 537–556.
- Svoray, T., Shoshany, M., 2003. Herbaceous biomass retrieval in habitats of complex composition: a model merging SAR images with unmixed landsat TM data. *IEEE Trans. Geosci. Rem. Sens.* 41, 1592–1601.
- Svoray, T., Shoshany, M., 2004. Multi-scale analysis of intrinsic soil factors from SAR-based mapping of drying rates. *Rem. Sens. Environ.* 92, 233–246.

- Tayfur, G., Singh, V.P., 2006. ANN and Fuzzy Logic Models for Simulating Event-Based Rainfall-Runoff. *J. Hydrol. Eng.*, ASCE 132, 1321–1329.
- Tayfur, G., Ozdemir, S., Singh, V.P., 2003. Fuzzy logic algorithm for runoff-induced sediment transport from bare soil surfaces. *Adv. Water Res.* 26, 1249–1256.
- Thornes, J.B., 1980. Erosional processes of running water and their spatial and temporal controls: a theoretical viewpoint. In: Kirkby, M.J., Morgan, R.P.C. (Eds.), *Soil Erosion*. John Wiley & Sons, New York, pp. 129–182.
- Tran, L.T., Ridgley, M.A., Duckstein, L., Sutherland, R., 2002. Application of fuzzy logic-based modelling to improve the performance of the revised universal soil loss equation. *Catena* 47, 203–226.
- Trimble, S.W., Crosson, P., 2000. Measurements and models of soil loss rates – response. *Science* 290, 1301.
- Tucker, C.J., 1979. Red and photographic infrared linear combinations for monitoring vegetation. *Rem. Sens. Environ.* 8, 127–150.
- Tucker, G.E., Lancaster, S.T., Gasparini, N., Bras, M.R.L., Rybarczyk, S.M., 2001. An object-oriented framework for distributed hydrologic and geomorphic modelling using triangulated irregular networks. *Comput. Geosci. UK* 27, 959–973.
- Tucker, G.E., Slingerland, R.L., 1994. Erosional dynamics, flexural isostasy, and long-lived escarpments – a numerical modelling study. *J. Geophys. Res. Solid Earth* 99, 12229–12243.
- USDA-SCS, 1985. *National Engineering Handbook, Section 4 – Hydrology*. US Department of Agriculture, Soil Conservation Service, Washington, DC.
- Urbanski, J.A., 1999. The use of fuzzy sets in the evaluation of the environment of coastal waters. *Int. J. Geogr. Inf. Sci.* 13, 723–730.
- Valmis, S., Dimoyiannis, D., Danalatos, N.G., 2005. Assessing interrill erosion rate from soil aggregate instability index, rainfall intensity and slope angle on cultivated soils in central Greece. *Soil Till. Res.* 80, 139–147.
- Van Rompaey, A.J.J., Verstraeten, G., Van Oost, K., Govers, G., Poesen, J., 2001. Modelling mean annual sediment yield using a distributed approach. *Earth Surf. Proc. Land.* 26, 1221–1236.
- Willgoose, G.R., Bras, R.L., Rodriguez-Iturbe, I., 1991. Results from a new model of river basin evolution. *Earth Surf. Proc.* 16, 237–254.
- Wischmeier, W.H., Smith, D.D., 1978. *Predicting Rainfall Erosion Losses: A Guide to Conservation Planning*. Handbook, 537. United States Department of Agriculture (USDA), Washington DC.
- Yair, A., Kossovsky, A., 2002. Climate and surface properties: hydrological response of small and semi-arid watersheds. *Geomorphology* 42, 43–57.
- Zhu, A.X., Band, L.E., Dutton, B., Nimlos, T.J., 1996. Automated soil inference under fuzzy logic. *Ecol. Modell.* 90, 123–145.